Transactions, SMiRT-23
Manchester, United Kingdom - August 10-14, 2015
Division II

J-integral fracture toughness assessment of specimens containing dissimilar metal welds

Igor Simonovski[1], Martin Oliver[1], Myriam Bourgeois[2], Malik Aït-Bachir[3], Szávai Szabolcs[4], Robert Beleznai[4], Oriol Costa Garrido[5], Leon Cizelj[5], Sébastien Blasset[6], Erwan Jourden[7], Carlos Cueto-Felgueroso García[8], Guillermo Lopez Quesada[8]

[1] European Commission, DG JRC, Institute for Energy and Transport, The Netherlands
[2] CEA, DEN, DM2S, SEMT, LISN, France
[3] EDF - DIN - SEPTEN, Division RE (Réacteur nucléaire et Echangeurs) - Groupe TM (Thermo-Mécanique), Villeurbanne, France
[4] Bay Zoltán Nonprofit Ltd. for Applied Research, Institute for Logistics and Production Engineering, Hungary
[5] Jozef Stefan Institute, Reactor Engineering Division, Slovenia
[6] AREVA GmbH, PTCMF-G, Materials, Plant Life Management, Fracture Mechanics - Safety Analysis, Germany
[7] AREVA, Engineering and Project Organization (E&P), Mechanical Engineering: Structural Analysis (PEELS-F), France
[8] TECNATOM, Ingeniera de Componentes, Dirección Servicios Inspección y Pruebas, Spain

ABSTRACT

In 2012 a research project MULTIMETAL was started within the 7th Framework Programme for Research and Technological Development of the European Union. The aim of the project is to develop a standard for measuring the fracture resistance of multi-metallic specimen and the development of harmonized procedures for dissimilar metal welds (DMWs) brittle and ductile integrity assessment. DMWs connect ferritic and austenitic stainless steels and are present at a number of locations in light water reactors primary piping systems. In this paper the computations of J-integral and η_{pl}, performed within a benchmark 'Numerical Analyses of DMW Behaviour' are presented. CT, SEN(B) and SEN(T) specimens, containing various DMW material zones, are used. In general, the best agreement is obtained for the CT specimens, followed by the SEN(B) and SEN(T) specimens.

INTRODUCTION

At the moment there is no existing standard for the fracture resistance testing of multi-metallic components or specimens that are made up of different material sections joined together via a weld. Existing standards for fracture resistance testing like ASTM E1820-13 ASTM (2013), ISO 12135:2002 ISO (2002) and engineering procedures or schemes like DNV DNV (2006) for the estimation of J-integral values are intended for specimens made of homogeneous material only. Thus in early 2012 a group of 11 European organisations started a R&D project MULTIMETAL MULTIMETAL (2012) with the aim of filling the above gaps. The objectives of the project are the development of a standard for fracture resistance testing of multi-metallic specimens and the development of harmonized procedures for dissimilar metal welds (DMWs) brittle and ductile integrity assessment. DMWs are typically present in safe-ends of LWRs primary circuits.

The underlying aim of MULTIMETAL is to provide recommendations for a good practice approach for the integrity assessment of DMWs as part of overall integrity analyses and leak-before-break (LBB) procedures. The project was funded by the European Commission (EC) within its 7th Framework Program and concluded in January 2015. This paper presents a part of the results obtained within the numerical benchmark: 'Numerical Analyses of DMW Behaviour'. Within the benchmark J-integral and η_{pl} values were computed for CT, SEN(B) and SEN(T) specimens containing various DMW material zones.

MOCK-UPS AND SPECIMENS

Specimens based on two mock-ups were used in the benchmark. Mock-ups are representative of DMWs from operating NPPs in terms of geometry, material and weld procedure. They consist of an austenitic stainless steel plate, a ferritic steel plate and a weld between the two plates, see Fig. 1. Mock-up1 (MU1) is a narrow gap, no buttering weld with Inconel 52 as filler material and resembles a weld in the primary circuit of the European Pressurized Water Reactor (EPR). This mock-up continues the work of the STYLE STYLE

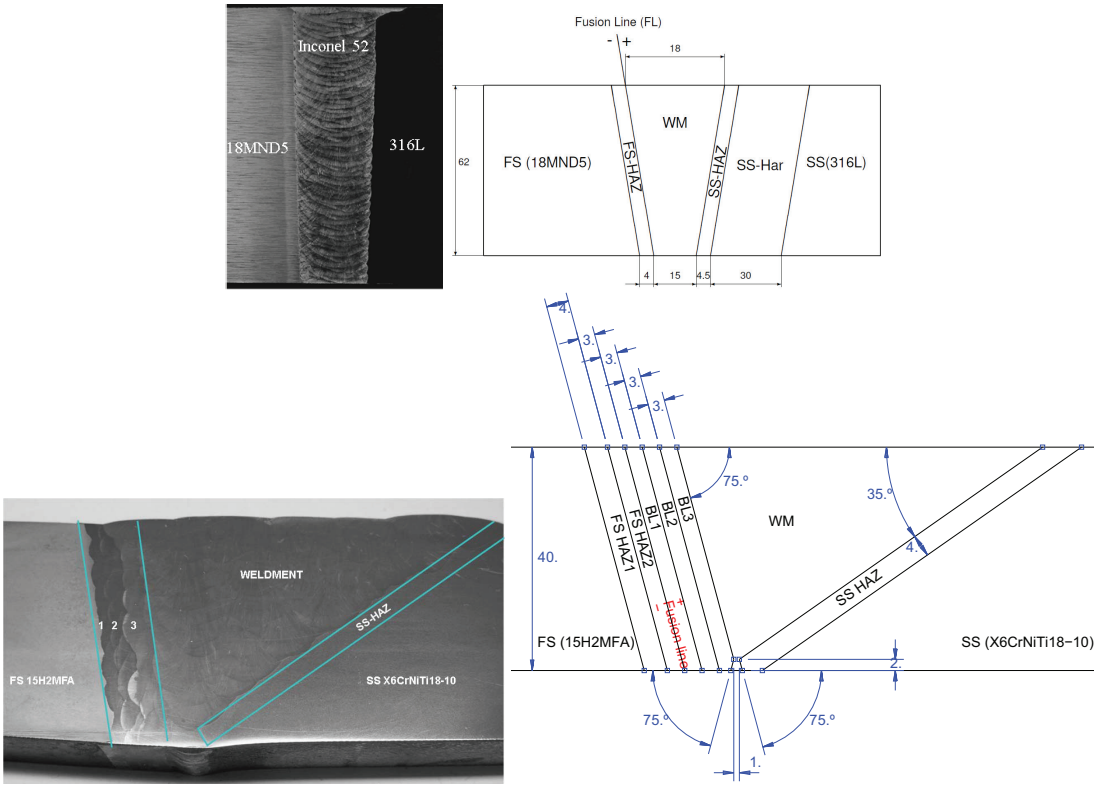

Figure 1: MU1 (top) and MU3 (bottom). All the dimensions are in mm.

(2010) and ADIMEW Faidy (2015) projects that dealt with improving the LBB assessment procedures for DMWs. MU3 resembles a DMW in primary circuits of VVER-440 reactors. It is composed of a 15H2MFA ferritic steel plate, two heat affected zones on the ferritic side, three buttering layers, weld, heat affected zone on the stainless steel side and the X6CrNiTi18-10 stainless steel plate. Post-weld heat treatment has been performed on all the mock-ups. An extensive material characterization of the mockups has been performed Bourgeois et al. (2015a,b,c); Keinänen et al. (2015). Fig. 2 shows the corresponding room-temperature stress-strain data for different materials. Adjacent materials have different yield stresses and hardening

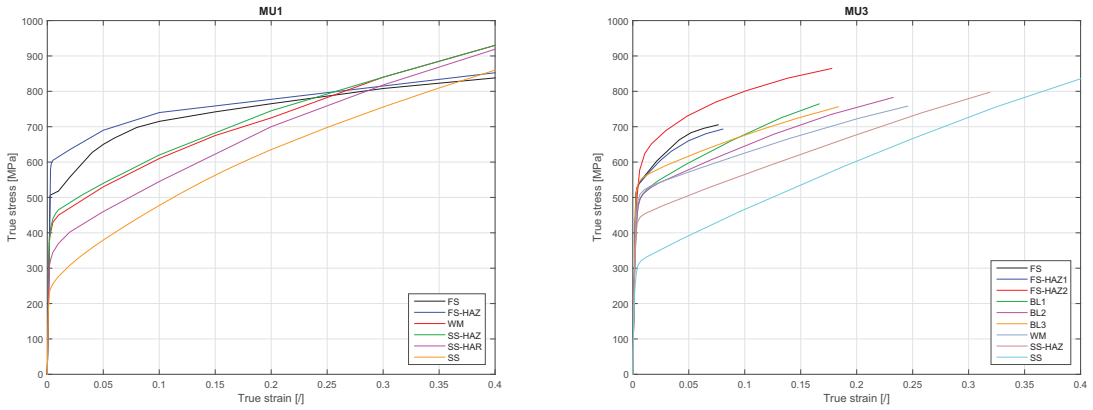

Figure 2: True stress-strain curves for different materials in the MU1 and MU3.

which affects the strain concentrations and results in unsymmetrical response of the fracture specimens. CT, SEN(B) and SEN(T) specimens were cut out of the mock-ups. In case of MU1 specimens, the crack is usually placed on the fusion line between the FS-HAZ and WM or slightly inside the WM. This is based on the STYLE and ADIMEW studies which showed that this interface is the weakest area in terms of toughness Bourgeois et al. (2015c).

NUMERICAL ANALYSIS

J-integral and η_{pl} values were calculated for a matrix of 2D cases with different crack positions, see Table 1. In addition, a smaller number of 3D cases was also computed, however, those are not covered here. For each case three crack lengths were used: a/W=0.5, 0.6 and 0.7. The cases were distributed between the participants in a way that at least two participants computed each case. Global model behaviour was checked by comparing Load-Load-Line-Displacement(LLD)/Crack-Mouth-Opening-Displacement(CMOD) responses.

J-integral values were computed using finite element (FE) analyses. The original J-integral definition is valid only for homogeneous materials and is path independent. For inhomogeneous materials a contribution due to the material inhomogeneity (C_{inh}) needs to be added, Eq. (1) Brocks and Scheider (2001); Kikuchi and Miyamoto (1982). However, if the phase boundary between the two materials is parallel to the crack line, the additional contribution C_{inh} becomes zero Brocks and Scheider (2001); Kolednik et al. (2005); Simha et al. (2003). This is true in all our cases. One needs to make sure that the contours don't cross further away interfaces that are not parallel to the crack line.

$$J_i = J_{homog} + C_{inh} = \underbrace{\oint_{\Gamma} [wn_i - \sigma_{ij} n_k u_{j,i}]\, ds}_{J_{homog}} \underbrace{- \oint_{\Gamma_{pb}} [wn_i - \sigma_{ij} n_k u_{j,i}]\, ds}_{C_{inh}} \tag{1}$$

The computed J-integral values were split into elastic and plastic part, Eq. (2), in line with ASTM E1820-13 ASTM (2013). η_{pl} dimensionless correction factors were then computed. The following definition of LLD values were used for computing η_{pl} values: CT-opening of the crack at the LLD line, SEN(B)-displacement of the point underneath the top pin and SEN(T)-opening of the crack at the bottom edge of the specimen.

$$J = J_{el} + J_{pl}, \qquad J_{pl} = \frac{\eta_{pl} A_{pl}}{B_N b_o}, \qquad \eta_{pl} = \frac{J_{pl} B_N b_o}{A_{pl}} \tag{2}$$

Initial validation of the models was performed by comparing J-integral and η_{pl} values using homogeneous cases with only ferritic steel 18MND5 material properties Simonovski et al. (2014). Following this, different material zones were introduced into the specimens, Figs. 3 and 4.

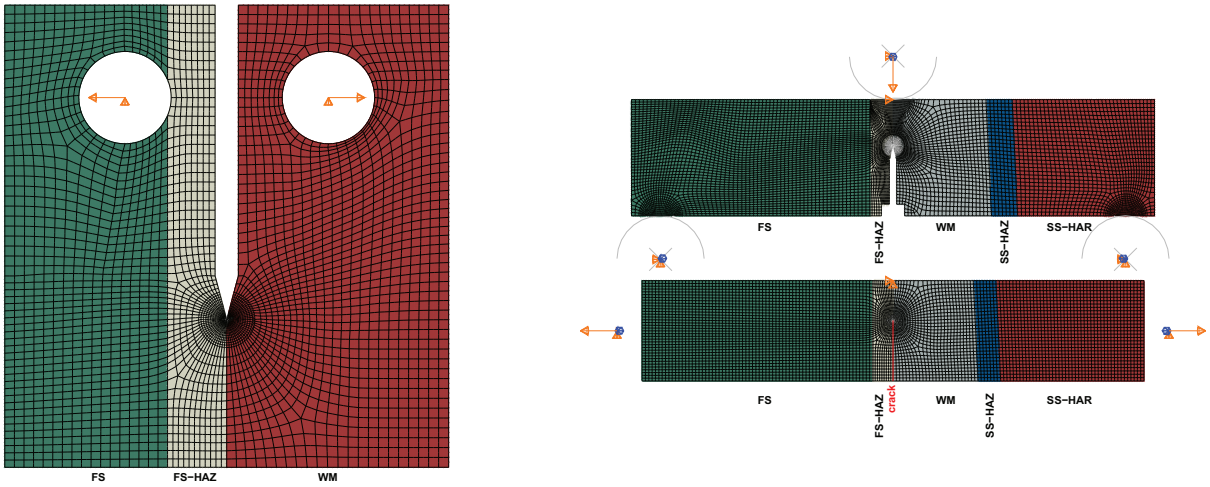

Figure 3: MU1 material zones for CT, SEN(B) and SEN(T) specimens.

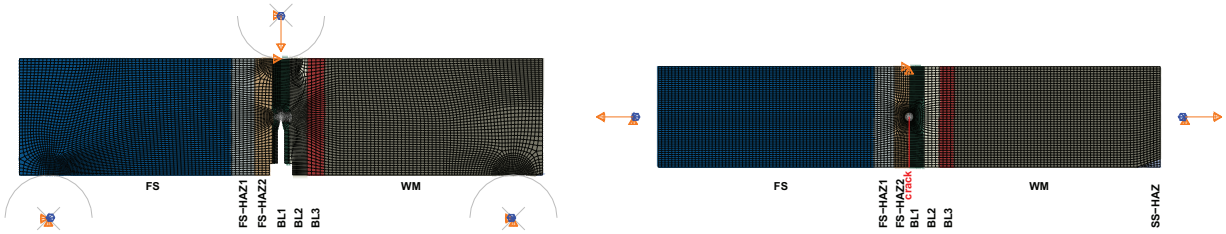

Figure 4: MU3 material zones for SEN(B) and SEN(T) specimens.

Boundary conditions

The boundary conditions were defined by the participants. For CT specimens the loads were applied by either linking displacements at the pin centers to the surrounding pin hole surfaces or by explicitly modelling pins and transferring the loads to the specimen through pin/specimen contacts. For SEN(B) the loads were applied by moving the top pin downwards and prescribing contact between the pin and the specimen. Most participants used frictionless contact, some applied a friction coefficient of 0.05. Clamped boundary conditions were needed to be specified for the SEN(T) specimen.

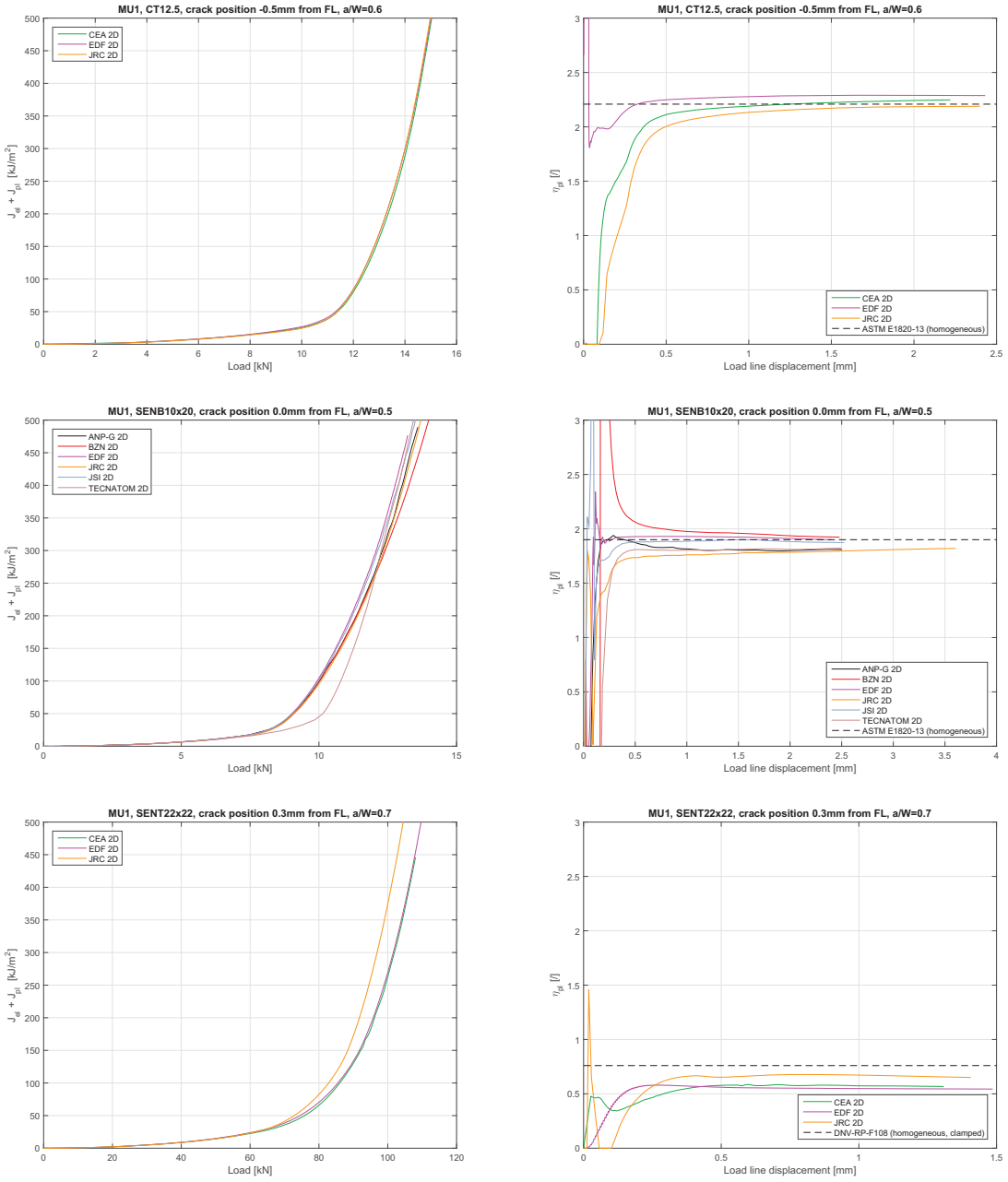

Figure 5: MU1. Top: CT12.5 a/W=0.6, crack position FL-0.5 mm. Middle: SEN(B)10x20, a/W=0.5, crack position at FL. Bottom: SEN(T)22x22, a/W=0.7, crack position FL+0.3 mm.

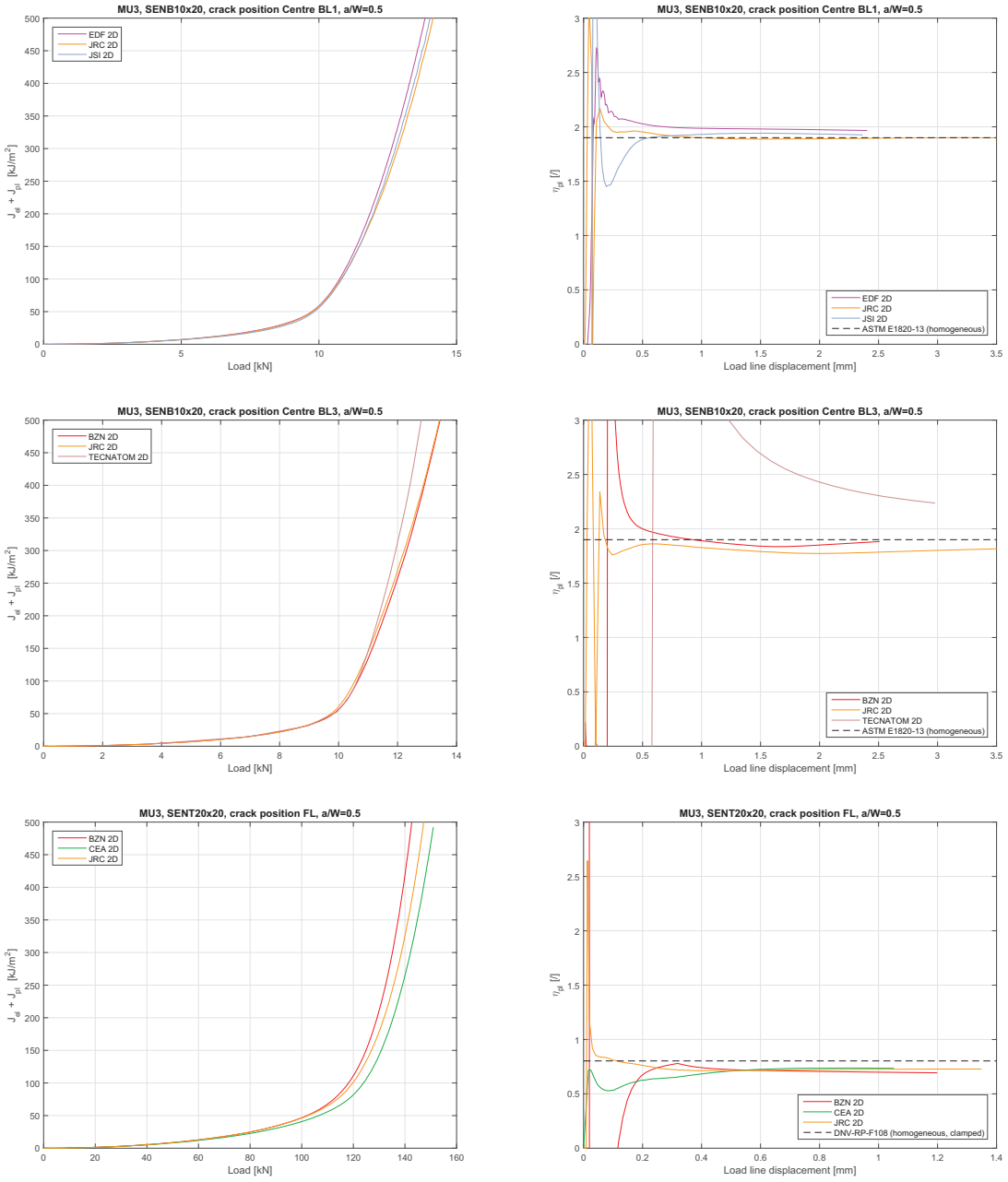

Figure 6: MU3. Top: SEN(B)10x20, a/W=0.5, crack position Centre BL1. Middle: SEN(B)10x20, a/W=0.5, crack position Centre BL3. Bottom: SEN(T)20x20, a/W=0.5, crack position FL.

Table 1: MU1 and MU3 2D cases.

MU1 (27 cases)	
Specimen type	Crack position [mm] from FL
CT12.5	0.0
	-0.5
CT25	0.0
SEN(B)20x20	0.5
SEN(B)10x20	0.0
	-0.5
SEN(T)22x22 (displ. contr.)	0.3
SEN(T)20x20 (displ. contr.)	0.0
	-0.5

MU3 (21 cases)	
Specimen type	Crack position [mm] from FL
SEN(B)10x20	FS-HAZ2 (-2 mm from FL)
	Centre BL1
	Centre BL2
	Centre BL3
	WM (2mm from border to BL3)
SEN(T)20x20 (displ. contr.)	FL
	Centre BL1

Table 2: MU1, comparison of η_{plLLD} values for the 2D cases.

Specimen type	Crack position [mm] from FL	a/W	ANP-F	ANP-G	BZN	CEA	EDF	JRC	JSI	TEC-NATOM	Average value	ASTM E1820-13 (homogeneous)	DNV-RP-F108 (homogeneous clamped)
CT12.5	0.0	0.5		2.1896		2.3105		2.2126			2.2376	2.2610	
		0.6				2.3084		2.2396	2.3066		2.2849	2.2088	
		0.7		2.1963				2.1726			2.1845	2.1566	
	-0.5	0.5		2.1998		2.2602	2.2044	2.1579			2.2056	2.2610	
		0.6				2.2475	2.2879	2.1888			2.2414	2.2088	
		0.7					2.2123	2.1287	2.1660		2.1690	2.1566	
CT25	0.0	0.5				2.3106		2.1736		2.2247	2.2363	2.2610	
		0.6				2.2900		2.2803		2.2743	2.2815	2.2088	
		0.7				2.2303		2.1965		2.2164	2.2144	2.1566	
SENB20x20	0.5	0.5		1.8669			1.9175	1.8856			1.8900	1.9000	
		0.6					1.9565	1.9779			1.9672	1.9000	
		0.7					1.9958	2.0113		2.0415	2.0162	1.9000	
SENB10x20	0.0	0.5		1.8085	1.9244		1.9005	1.8134	1.8742	1.8193	1.8567	1.9000	
		0.6						1.9070	1.9762	1.9098	1.9310	1.9000	
		0.7						1.9675	2.0284	2.0101	2.0020	1.9000	
	-0.5	0.5					1.8827	1.7704	1.8094		1.8208	1.9000	
		0.6					1.9091	1.8435	1.8560	1.8858	1.8736	1.9000	
		0.7					1.9412	1.9079	1.9422	1.9287	1.9300	1.9000	
SENT22x22	0.3	0.5				0.7414	0.7455	0.7898			0.7589		0.8029
		0.6				0.6257	0.6199	0.6854			0.6437		0.7794
		0.7				0.5683	0.5443	0.6517			0.5881		0.7601
SENT20x20	0.0	0.5	0.7100	0.7055				0.7333			0.7163		0.8029
		0.6	0.6079		0.5981			0.6581			0.6214		0.7794
		0.7	0.5745	0.7780				0.6745			0.6757		0.7601
	-0.5	0.5	0.7040	0.8749				0.7138			0.7642		0.8029
		0.6	0.6018					0.6279			0.6149		0.7794
		0.7	0.5666					0.6417			0.6042		0.7601

Results

The analyses were performed under small displacement and plain strain conditions. True stress-true strain curves as indicated in Fig. 2 were applied. Figs. 5 and 6 show an excerpt of the results. Good agreement amongst the participants was obtained for global model responses, J-integral-load and η_{pl} values for all cases listed in Table 1. These are all 2D cases. In general the best agreement in global response was obtained for the CT specimens, followed by the SEN(B) and SEN(T) specimens. The agreement of the results for 3D cases (both MU1 and MU3) was not satisfactory and those results were considered as unreliable Simonovski and Martin (2015). The calculated η_{pl} values are listed in Tables 2 and 3. In some cases the calculated η_{pl} values differed somewhat even if the global responses and J-integral-load values were very similar, see Fig. 5 top part. On the other hand, there were instances where global responses

and J-integral-load values differed somewhat but the computed η_{pl} values were almost identical, see Fig. 6 bottom part. The reason is probably due to the fact that the η_{pl} is affected by both the J_{pl} (nominator) and A_{pl} (denominator) contributions, Eq. (2), and there are instances where the differences cancel each other out. For any final η_{pl} values a benchmark for verifying the η_{pl} computation procedure should be done first where the η_{pl} is computed from a set of given LLD-Load and J-integral-load curves.

Table 3: MU3, comparison of η_{plLLD} values for the 2D cases.

Specimen type	Crack position [mm] from FL	a/W	BZN	CEA	EDF	JRC	JSI	TEC-NATOM	VTT	Average value	ASTM E1820-13 (homogeneous)	DNV-RP-F108 (homogeneous clamped)
SENB10x20	FS-HAZ 2, -2mm from FL	0.5			1.8760	1.7620	1.7410			1.7930	1.9000	
		0.6			1.8789	1.8220	1.7942			1.8317	1.9000	
		0.7			1.8806	1.8573	1.8440			1.8606	1.9000	
	Centre BL1	0.5			1.9666	1.8990	1.9272			1.9309	1.9000	
		0.6			1.9979	1.9654	2.0006			1.9880	1.9000	
		0.7			2.0296	2.0154	2.0268	2.0505		2.0306	1.9000	
	Centre BL2	0.5	1.9965			1.9255			1.9600	1.9607	1.9000	
		0.6	2.0398			1.9759				2.0078	1.9000	
		0.7	2.0589			2.0188				2.0389	1.9000	
	Centre BL3	0.5	1.8803			1.8152		2.2633		1.9863	1.9000	
		0.6	1.9464			1.8776		2.0261		1.9500	1.9000	
		0.7	1.9813			1.9151		1.9235		1.9400	1.9000	
	Weld (2mm from BL3 border)	0.5	1.9335			1.8809				1.9072	1.9000	
		0.6	2.0421			1.9797				2.0109	1.9000	
		0.7	2.0640			2.0193				2.0416	1.9000	
SENT20x20	FL	0.5	0.6945	0.7355		0.7283				0.7194		0.8029
		0.6		0.6927		0.7008				0.6968		0.7794
		0.7	0.4347	0.7016		0.7462				0.6275		0.7601
	Centre BL1	0.5		0.7520		0.7399		0.8798		0.7906		0.8029
		0.6		0.7167		0.7235				0.7201		0.7794
		0.7				0.7702				0.7702		0.7601

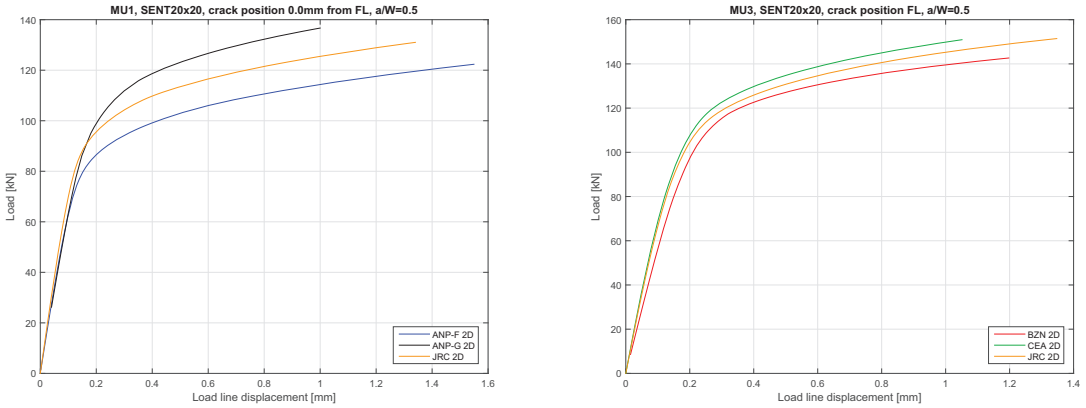

Figure 7: Global responses of SEN(T)20x20 cases, a/W=0.5, crack at FL. Left: MU1. Right: MU3.

The average η_{pl} values for MU1 CT specimens are up to the first digit equal to the ASTM E1820-13 ASTM (2013) homogeneous values. In the homogeneous case η_{pl} values decrease monotonically with higher a/W ratio whereas in the multi-metallic cases the highest average η_{pl} values are obtained at a/W=0.6. For SEN(B) cases average η_{pl} values monotonically increase with higher a/W ratios for both MU1 and MU3. A slight exception to this is the MU3, crack at centre BL3 case, which is influenced by the non-stabilized TECNATOM η_{pl} value, see Fig. 6 middle part. SEN(T) cases resulted in the largest relative differences in computed η_{pl} values, both for the MU1 and MU3 cases, see Fig. 7. The reason for this is probably in different implementations of the clamped boundary conditions. Different global responses were obtained for MU1 SEN(T)22x22 and even more so for the MU1 SEN(T)20x20 cases. Global responses of MU3 SEN(T)

cases were closer to each other (compared to the MU1), with the exception when the crack was placed at FL, a/W=0.7. BZN result in this case deviated significantly from the other two, see Table 3.

CONCLUSIONS

J-integral fracture toughness and η_{pl} calculations were performed for EPR and VVER-440 nuclear-grade welds between ferritic and austenitic stainless steel plates. Computations were performed on standard CT, SEN(B) and SEN(T) specimens, each containing various dissimilar metal weld material zones. A compendium of η_{pl} values, covering different specimens, crack positions and lengths was created. The computations were performed as a round-robin exercise within the MULTIMETAL project of the European Commission's 7th Framework Program.

In general, the best agreement was obtained for the CT specimens, followed by the SEN(B) and SEN(T) specimens. In some cases the calculated η_{pl} values differed somewhat even if the global responses and J-integral-load values were very similar. On the other hand, there were instances where global responses and J-integral-load values differed somewhat but the computed η_{pl} values were almost identical. For any final η_{pl} values a benchmark for verifying the η_{pl} computation procedure should be done first. SEN(T) cases resulted in the largest relative differences in computed η_{pl} values, both for the MU1 and MU3 cases. The reason for this is probably in the different implementations of the clamped boundary conditions which resulted in different global responses of the models.

ACKNOWLEDGMENTS

This project has received funding from the European Community's Seventh Framework Program (FP7/2012-2015) under grant agreement n°295968.

REFERENCES

ASTM. *Standard Test Method for Measurement of Fracture Toughness. E1820-13*. American Society for Testing and Materials (ASTM), 2013.

M. Bourgeois, O. Ancelet, and S. Chapuliot. Elasto-plastic properties in dissimilar metal weld junctions: Stress-strain curves determination for constitutive materials. In *Proceedings of the ASME 2015 Pressure Vessels and Piping Conference*. ASME, 2015a.

M. Bourgeois, O. Ancelet, G. Perez, P. Rózsahegyi, S. Szávai, and S. Lindqvist. MULTIMETAL Deliverable D3.6, Mechanical Behaviour Identification. Technical report, CEA, BZF, VTT, January 2015b.

M. Bourgeois, G. Perez, and S. Chapuliot. Fracture properties in dissimilar metal weld junctions: Experimental methodology of characterization. In *Proceedings of the ASME 2015 Pressure Vessels and Piping Conference*. ASME, 2015c.

W. Brocks and I. Scheider. Numerical aspects of the path-dependence of the J-integral in incremental plasticity. how to calculate reliable J-values in FE analyses. Technical report, Institut fur Werkstofforschung GKSS-Forschungszentrum Geesthacht, 2001.

DNV. *Recommended practice DNV-RP-F108. Fracture control for pipeline installation methods introducing cyclic plastic strain*. DET NORSKE VERITAS (DNV), 2006.

C. Faidy. Structural integrity of dissimilar welds: ADIMEW project overview (http://dx.doi.org/10.1115/pvp2004-2540). In *Proceedings of the ASME 2004 Pressure Vessels and Piping Conference*. ASME, 2015.

ISO. *ISO 12135:2002 Metallic materials - Unified method of test for the determination of quasistatic fracture toughness*. International Organization for Standardization (ISO), 2002.

H. Keinänen, P. Karjalainen-Roikonen, P. Gilles, E. Keim, S. Blasset, and T. Nicak. Results of EC FP7 structural performance of multi-metal component project: Dissimilar metal weld fracture resistance investigation. In *Proceedings of the ASME 2015 Pressure Vessels and Piping Conference*. ASME, 2015.

M. Kikuchi and H. Miyamoto. Evaluation of J_k integrals for a crack in multiphase materials. *Recent Research on Mechanical Behavior of Materials, Bulletin of Fracture Mechanics Laboratory*, 1, 1982.

O. Kolednik, J. Predan, G.X. Shan, N.K. Simha, and F.D. Fischer. On the fracture behavior of inhomogeneous materials-a case study for elastically inhomogeneous bimaterials. *International Journal of Solids and Structures*, 42(2):605–620, January 2005.

MULTIMETAL. 'Structural performance of multi-metal component' (http://projects.tecnatom.es/webaccess/multimetal), 2012.

N.K. Simha, F.D. Fischer, O. Kolednik, and C.R. Chen. Inhomogeneity effects on the crack driving force in elastic and elastic-plastic materials. *Journal of the Mechanics and Physics of Solids*, 51(1):209–240, January 2003.

I. Simonovski and O. Martin. MULTIMETAL Deliverable D4.2: J Value Estimation of Different Multi-Metallic Specimen Designs. Technical report, European Commission, Joint Research Centre (JRC), Institute for Energy and Transport, 2015.

I. Simonovski, O. Martin, and G. Machina. MULTIMETAL WP4.2: WP4.2 'K/J Value Estimation of different Specimen Designs' Part 1: Homogeneous Specimens. Technical report, European Commission, Joint Research Centre (JRC), Institute for Energy and Transport, 2014.

STYLE. 'Structural integrity for lifetime management-non rpv components', grant agreement no 249648, 2010.